Computational Studies of Structures and Properties of Metallaboranes. 2. Transition-Metal Dicarbollide Complexes

Michael Bühl,*,† Josef Holub,‡ Drahomír Hnyk,‡ and Jan Macháček‡

Max-Planck-Institut für Kohlenforschung, Kaiser-Wilhelm-Platz 1, D-45470 Mülheim an der Ruhr, Germany, and Institute of Inorganic Chemistry, Academy of Sciences of the Czech Republic, CZ-250 68 Řež near Prage, Czech Republic

Received November 30, 2005

A density functional study at the BP86 level is presented for metal bis(dicarbollides), $[3\text{-M-}(1,2\text{-}C_2B_9H_{11})_2]^n$ (M/n = Fe,Ru/2−, Co,Rh/1−, Ni,Pd/0), as well as selected mixed- and half-sandwich complexes $[3\text{-M(L)-}(1,2\text{-}C_2B_9H_{11})]$ {M(L) = Fe($C_6H_3Me_3$), Ru(C_6H_6), Ru(CO)$_3$, Rh(C_5Me_5)}. Available experimental ^{11}B NMR chemical shifts of these complexes with *closo* structure of the metallacarborane moiety are reproduced reasonably well at the GIAO-B3LYP/II′ level, with mean absolute deviations of ca. 3 ppm (over a chemical-shift range of ca. 50 ppm). The potential usefulness of this computational protocol for assignments and structural refinements of transition-metal-containing heteroboranes is illustrated in an application to 14-vertex *closo* clusters $[1,14\text{-}\{(\text{arene})\text{Ru}\}_2(x,y\text{-}C_2B_{10}H_{12})$, where the C-substitution pattern in the carborane moiety is identified.

1. Introduction

The sandwich structure of ferrocene is one of the most fruitful paradigms in organometallic chemistry.[1] It is a model not only for a plethora of metallocenes[2] but also for the even larger family of "mixed-" and "half-sandwich" complexes. Isolobal replacement of the cyclopentadienyl ligand with various *nido* borane and heteroborane clusters that contain open pentagonal faces affords a yet wider variety of ferrocene-like "full-, mixed-, or half-sandwich" metallaheteroboranes, which were recently reviewed by Štíbr.[3] The bonding between the sandwiched metal and its heteroborane ligands resembles that in ferrocene to a large degree.[4] X-ray crystallography is the predominant means for structural characterization of such complexes.[5] The structures of the bare *nido*-heteroborane ligands, as well as those of other polyhedral boranes and their derivatives, can in addition (or alternatively) be refined by employing the joint experimental and computational ab initio/GIAO/NMR method.[6,7] In this approach, geometries and ^{11}B chemical shifts of all possible candidates for a given compound are computed at suitable ab initio levels, and the structure that gives best accord with the experimentally observed chemical shifts is taken as the best representation of the compound under scrutiny. The credibility of structural assigments based on this method has been attested to "rival that of X-ray crystallography".[8]

Theoretical ^{11}B chemical shift calculations for metallaboranes are scarce and have so far been mostly applied for interpretative purposes in the context of the electronic structure of such complexes.[9] We have recently studied an archetypical metallacarborane, cobalt bis(dicarbollide), $[3\text{-Co-}(1,2\text{-}C_2B_9H_{11})_2]^-$, **1**,[10] the molecular geometry and conformational properties of which were derived from density functional theory (DFT) using a well-established functional, BP86. The observed ^{11}B chemical shifts of **1** were reproduced with a reasonable accuracy at the GIAO-B3LYP/II′ level, suggesting that this particular combination of DFT levels would be suitable for metallacarboranes in general. We now present a systematic performance test for a larger set of such complexes in order to check the validity of this assumption.

A natural choice of target complexes is the extension of the above study of **1** to isoelectronic sandwiches of the type $[M(C_2B_9H_{11})_2]^n$,[11−13] replacing the Co(III) center with its corresponding neighbors in the periodic table, viz., Fe(II), Ni(IV), Ru(II), Rh(III), and Pd(IV) (see Scheme 1). Three of these

* To whom correspondence should be addressed. Fax: int. code + (0)-208-306 2996. E-mail: buehl@mpi-muelheim.mpg.de.

† Max-Planck-Institut für Kohlenforschung.

‡ Academy of Sciences of the Czech Republic.

(1) See for example: (a) Elschenbroich, C.; Salzer, A. *Organometallics*, 2nd ed.; VCH: Weinheim, 1992. (b) Special issue on the 50th anniversary of the discovery of ferrocene: Adams, R. D. *J. Organomet. Chem.* **2001**, *637*, 1.

(2) (a) Haaland, A. *Acc. Chem. Res.* **1979**, *11*, 415. (b) Haaland, A. Organometallic Compounds of Main Group Elements. In *Stereochemical Applications of Gas-Phase Electron Diffraction*; Hargittai, I., Hargittai, M., Eds.; VCH Publishers: New York, 1988; Part B, p 325.

(3) Štíbr, B. *J. Organomet. Chem.* **2005**, *690*, 2694.

(4) See for instance: Brown, D. A.; Fanning, M. O.; Fitzpatrick, N. J. *Inorg. Chem.* **1978**, *17*, 1620.

(5) Apart from Štíbr's review, the most recent studies include: (a) Bakardjiev, M.; Holub, J.; Carr, M.; Kennedy, J. D.; Štíbr, B. *J. Chem. Soc., Dalton Trans.* **2005**, 909. (b) Holub, J.; Grüner, B.; Perekalin, D. S.; Golovanov, D. G.; Lyssenko, K. A.; Petrovskii, P. V.; Kudinov, A. R.; Štíbr, B. *Inorg. Chem.* **2005**, *44*, 1655. (c) Perekalin, D. S.; Lysenko, K. A.; Petrovskii, P. V.; Holub, J.; Štíbr, B.; Kudinov, A. R. *J. Organomet. Chem.* **2005**, *690*, 2775. (d) Perekalin, D. S.; Holub, J.; Golovanov, D. G.; Lysenko, K. A.; Petrovskii, P. V.; Štíbr, B.; Kudinov, A. R. *Organometallics* **2005**, *24*, 4387.

(6) (a) Bühl, M.; Schleyer, P. v. R. *J. Am. Chem. Soc*. **1992**, *114*, 477. (b) Review: Bühl, M. In *Encyclopedia of Computational Chemistry*; Schleyer, P. v. R., Allinger, N. L., Kollman, P. A., Clark, T., Schaefer, H. F., Gasteiger, J., Schreiner, P. R., Eds.; Wiley: Chichester, 1998; p 1835.

(7) For the most recent applications of the ab initio(DFT)/GIAO/NMR method in this area see for example: (a) Štíbr, B.; Holub, J.; Bakardjiev, M.; Hnyk, D.; Tok, O. L.; Milius, W.; Wrackmeyer, B. *Eur. J. Inorg. Chem.* **2002**, 2320. (b) Bakardjiev, M.; Holub, J.; Štíbr, B.; Hnyk, D.; Wrackmeyer, B. *Inorg. Chem.* **2005**, *44*, 5826, and references therein.

(8) Onak, T.; Tseng, J.; Diaz, M.; Tran, D.; Arias, J.; Herrera, S.; Brown, D. *Inorg. Chem.* **1993**, *32*, 487.

(9) See for instance: (a) Fehlner T. P. *Collect. Czech. Chem. Commun.* **1999**, *64*, 767. (b) Le Guennic, B.; Jiao, H.; Kahlal, S.; Saillard, J. Y.; Halet, J. F.; Ghosh, S.; Shang, M.; Beatty, A. M.; Rheingold, A. L.; Fehlner, T. P. *J. Am. Chem. Soc*. **2004**, *126*, 3203.

(10) Bühl, M.; Hnyk, D.; Macháček, J. *Chem. Eur. J.* **2005**, *11*, 4109.

(11) Review of Ni and Fe bis(dicarbollides): Sivaev, I. B.; Bregadze, V. I. *J. Organomet. Chem.* **2000**, *614*, 27.

(12) Review of Co bis(dicarbollide): Sivaev, I. B.; Bregadze, V. I. *Collect. Czech. Chem. Commmun.* **1999**, *64*, 783.

10.1021/om051025f CCC: $33.50
Publication on Web 03/21/2006

Scheme 1. Skeletal Structure and Numbering Scheme of $[M(C_2B_9H_{11})_2]^n$ [a]

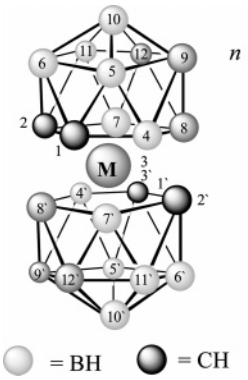

M / *n*		
Fe / 2-	Co / 1-	Ni / 0
(2)	**(1)**	**(3)**
Ru / 2-	Rh / 1-	Pd / 0
(4)	**(5)**	**(6)**

[a] B and C atoms in light and dark gray, respectively; H atoms not shown.

are known experimentally,[14] namely, the dianionic iron complex,[15] as well as the neutral Ni and Pd species.[16] [3-Ni-(1,2-$C_2B_9H_{11})_2$] (**3**) has attracted recent interest because one-electron reduction leads to a formal Ni(III) species with a different mutual orientation of the two dicarbollide ligands, and control of the concomitant rotational and oscillatory motion of the sandwich around the molecular axis could form the basis for the possible construction of the smallest nanomachines.[17]

We focus on the accuracy of the computed ^{11}B chemical shifts in these bis(dicarbollides) and related half-sandwich metal-dicarbollide complexes. As it turns out, the performance of the DFT protocol for this test set is comparable to that for the prototypical **1**, as far as the mean absolute deviation from experiment is concerned. Occasional larger errors for individual sites notwithstanding, this accuracy can be sufficient for structural applications. As an illustration of this point, we include a case study of a 14-vertex metallacarborane, a topical area of research in boron chemistry.

2. Computational and Experimental Details

Stationary points were optimized at the BP86 level, i.e., employing the exchange and correlation functionals of Becke[18] and Perdew,[19] respectively, together with a fine integration grid (75 radial shells with 302 angular points per shell), and a basis set consisting of the augmented Wachters' basis[20] on the 3d metals (8s7p4d, full contraction scheme 62111111/3311111/3111), (6s5p3d) valence basis sets together with the corresponding small-core Stuttgart−Dresden relativistic effective core potentials (ECPs) on the 4d metals, and 6-31G* basis on all other elements.[21] This and comparable DFT levels have proven quite successful for transition-metal compounds and are well suited for the description of structures, energies, barriers, etc.[22] The nature of the stationary points was verified by computations of the harmonic frequencies at that level. Transition states were characterized by a single imaginary frequency, and visualization of the corresponding vibrational modes ensured that the desired minima are connected. Unless otherwise noted, energies are reported at the BP86 level without zero-point corrections. For the bis(dicarbollide) rotamers, such corrections afforded only minor changes in relative energies, by ca. 1−2 kJ/mol. Natural population analysis[23] was performed at the B3LYP level. Optimized coordinates of each isomer (single rotamer only) are provided as Supporting Information.

Magnetic shieldings were computed for BP86 geometries employing gauge-including atomic orbitals (GIAOs),[24] the BP86 or the hybrid B3LYP[25,26] functionals, together with basis II′, which consists of the basis sets and ECPs on the metals as described above, a contracted (5s4p1d) Huzinaga basis of polarized triple-ζ quality on C and B, and a double-ζ basis (2s) on H.[27] For selected Ru and Rh complexes, GIAO-B3LYP/II′ calculations have been performed with a large all-electron basis set derived from Huzinaga and Klobukowski's even-tempered series on the metal (instead of the ECP); see ref 28 for details. This particular combination of density functionals and basis sets has proven to perform well for the computation of transition-metal chemical shifts[28,29] and for $\delta(^{11}B)$ values in cobalt bis(dicarbollide), **1**.[10]

^{13}C chemical shifts are reported relative to TMS, computed at the same level (B3LYP C shielding constant 181.1 ppm). ^{11}B chemical shifts have been calculated relative to B_2H_6 (B3LYP B shielding constant 81.4 ppm) and converted to the usual $BF_3{\cdot}OEt_2$ scale using the experimental $\delta(^{11}B)$ value of B_2H_6, 16.6 ppm.[30] Metal chemical shifts are reported relative to the metallocenes, with B3LYP shielding constants of −4503, 169, and 915 ppm for Fe-$(C_5H_5)_2$, Ru$(C_5H_5)_2$, and Rh$(C_5H_5)_2^+$, respectively (from the all-electron calculations). These computations were performed with the Gaussian 03 program.[31]

Additional NMR calculations were performed for the BP86-optimized geometries with the Amsterdam density functional code ADF[32,33] employing the BP86 functional. This functional has been successfully applied in many NMR computations involving heavy elements.[34] The two-component relativistic zeroth-order regular approximation (ZORA)[35] method including scalar and spin−orbit (SO)[36] corrections has been employed for the computations. We have used the triple-ξ basis set plus one polarization function for

(13) (a) Hawthorne, M. F.; Young, D. C.; Wegner, P. A. *J. Am. Chem. Soc.* **1965**, *87*, 1818. (b) Hawthorne, M. F.; Andrews, T. D. *J. Chem. Soc., Chem. Commun.* **1965**, 443.

(14) A large array of dicarbollide complexes bearing various substituents at the carborane moieties is also known. For a recent example see: Nuñez, R.; Tutusaus, O.; Teixidor, F.; Viñas, C.; Sillanpää, R.; Kivekäs, R *Chem. Eur. J.* **2005**, *11*, 5637.

(15) Hawthorne, M. F.; Warren, L. F., Jr.; Callahan, K. P.; Travers, N. F. *J. Am. Chem. Soc.* **1971**, *93*, 2407.

(16) (a) Warren, L. F.; Hawthorne, M. F. *J. Am. Chem. Soc.* **1967**, *89*, 470. (b) Warren, L. F.; Hawthorne, M. F. *J. Am. Chem. Soc.* **1970**, *92*, 1157.

(17) Hawthorne., M. F.; Zink, J. I.; Skeleton, J. M.; Bayer, M. J.; Liu, Ch.; Livshits, E.; Baer, R.; Neuhauser, D. *Science* **2004**, *303*, 1849.

(18) Becke, A. D. *Phys. Rev. A* **1988**, *38*, 3098−3100.

(19) (a) Perdew, J. P. *Phys. Rev. B* **1986**, *33*, 8822. (b) Perdew, J. P. *Phys. Rev. B* **1986**, *34*, 7406.

(20) (a) Wachters, A. J. H. *J. Chem. Phys.* **1970**, *52*, 1033. (b) Hay, P. J. *J. Chem. Phys.* **1977**, *66*, 4377.

(21) (a) Hehre, W. J.; Ditchfield, R.; Pople, J. A. *J. Chem. Phys.* **1972**, *56*, 2257. (b) Hariharan, P. C.; Pople, J. A. *Theor. Chim. Acta* **1973**, *28*, 213.

(22) See for instance: (a) Koch, W.; Holthausen, M. C. *A Chemist's Guide to Density Functional Theory*; Wiley-VCH: Weinheim, 2000, and the extensive bibliography therein. It should be noted that hybrid functionals such as B3LYP need not be superior to pure, gradient-corrected functionals, as far as geometries of transition-metal complexes are concerned. See for example: (b) Barden, C. J.; Rienstra-Kiracofe, J. C.; Schaefer, H. F. *J. Chem. Phys.* **2000**, *113*, 690. (c) Bühl, M.; Grigoleit, S. *Organometallics* **2005**, *24*, 1516.

(23) Reed, A. E.; Curtiss, L. A.; Weinhold, F. *Chem. Rev.* **1988**, *88*, 899.

(24) (a) Ditchfield, R. *Mol. Phys.* **1974**, *27*, 789. (b) Wolinski, K.; Hinton, J. F.; Pulay, P. *J. Am. Chem. Soc.* **1990**, *112*, 8251. (c) GIAO-DFT implementation: Cheeseman, J. R.; Trucks, G. W.; Keith, T. A.; Frisch, M. J. *J. Chem. Phys.* **1996**, *104*, 5497.

(25) Becke, A. D. *J. Chem. Phys.* **1993**, *98*, 5648.

(26) Lee, C.; Yang, W.; Parr, R. G. *Phys. Rev. B* **1988**, *37*, 785.

(27) Kutzelnigg, W.; Fleischer, U.; Schindler, M. In *NMR Basic Principles and Progress*; Springer-Verlag: Berlin, 1990; Vol. 23, pp 165−262.

(28) (a) Bühl, M. *Chem. Phys. Lett.* **1997**, *267*, 251. (b) Bühl, M.; Gaemers, S.; Elsevier, C. J. *Chem. Eur. J.* **2000**, *6*, 3272.

(29) Bühl, M. In *Calculation of NMR and ESR Parameters. Theory and Applications*; Kaupp, M., Bühl, M., Malkin, V. G., Eds.; Wiley-VCH: Weinheim, 2004; p 421.

(30) Onak, T. P.; Landesman, H. L.; Williams, R. E.; Shapiro, I. *J. Phys. Chem.* **1959**, *63*, 1533.

all atoms (denoted TZP) from the ADF library (^{11}B shielding constant of B_2H_6 with this approach: 79.1 ppm).

^{11}B and ^{13}C NMR spectra of [3-Ni-(1,2-$C_2B_9H_{11})_2$] were measured in Řež on a Varian Mercury Plus 400 NMR spectrometer under standard conditions on freshly prepared samples,[37] using deuterated acetone or chloroform as solvent. ^{13}C chemical shifts are given relative to TMS with the carbon signals of the deuterated lock solvents ($CDCl_3$ at $\delta = 77.0$ ppm and the methyl carbon of CD_3COCD_3 at $\delta = 29.8$ ppm) as internal reference; ^{11}B chemical shifts are given relative to $BF_3{\cdot}OEt_2$ and have been referenced to $(CH_3O)_3B$ (at $\delta = 18.1$ ppm) as external standard.

3. Results and Discussion

This part is organized as follows: Geometries, energetics, and chemical shifts of the symmetrical metal bis(dicarbollides) **1**−**6** are discussed in section 3.1. In section 3.2 these studies are extended to selected half-sandwich complexes containing one dicarbollide ligand, and an overall assessment of the theoretical ^{11}B chemical shift is given. An application of the computational approach to a structural question in the topical area of 14-vertex metallacarboranes is presented in section 3.3. For the dicarbollide ligand itself, only a single positional isomer with adjacent C atoms has been considered (namely, the 1,2-form as depicted in Scheme 1); see ref 10 for a comprehensive study of other positional isomers in the case of **1**. For the bis(dicarbollide) complexes, rotamers are identified by a suitable idealized dihedral angle given in the text.

3.1. Metal Bis(dicarbollides). The isoelectronic series **1**−**3** is well characterized, in terms of both ^{11}B NMR spectra and X-ray crystallography of suitable crystals.[38] From the 4d congeners **4**−**6**, to our knowledge, only the Pd derivative[16] has been reported.[39] For each compound, we have located all stationary points for rotation about the axis passing through B10 and B10′, using the dihedral angle B8′−M−B10−B8 (θ) as a measure for this rotation (see Scheme 1 for numbering). In all cases, minima are found for θ values equal or close to 180°, 108°, and 36° (labeled θ_{ideal} in Table 1), i.e., with a staggered conformation of the two dicarbollide ligands, whereas transition states are found for θ values near 0°, 72°, and 144°, i.e., with eclipsed ligands. Key geometrical parameters detailing the coordination environment about the metals in the minima are summarized in Table 1, together with experimental data, where available. For the Co derivative, where all three rotamers have been detected in the solid,[38c−e] only one representative example for each is given from the vast number of experimental structures. For the Fe[38a] and Ni[38e] complexes, only transoid ($\theta = 180°$) or cisoid structures ($\theta \approx 108°$), respectively, have been observed. In general, the optimized geometrical parameters agree reasonably well with the observed ones, with the tendency toward overestimation of metal−ligand bond lengths typical for the kind of density functional employed.[40]

Relative energies for all rotamers of **1**−**6** are summarized in Table 2. For the anions with M = Fe, Co, Ru, and Rh, the trans minimum is computed to be the most stable one, with the relative energies rising in the sequence 180° < 108° < 36°.[41] The opposite ordering is found for the two neutral complexes with M = Ni and Pd, for which the cisoid orientation with $\theta \approx 36°$ is lowest in energy.

In the absence of a polar environment (or counterions), the C_{2h} symmetric structures with $\theta = 180°$ would be expected to be preferred on electrostatic grounds, since they have no dipole moment. Those of the cisoid forms with $\theta \approx 36°$ are quite notable, ca. 5 D (BP86 level). In the case of **3**, this form appears to be stabilized by specific MO interactions, as illustrated for the HOMO in Figure 1. For **1**, the HOMO consists basically of an equatorial d-orbital at the metal, with some contributions from cluster-bonding, irrespective of the rotational angle

(31) Frisch, M. J.; Trucks, G. W.; Schlegel, H. B.; Scuseria, G. E.; Robb, M. A.; Cheeseman, J. R.; Montgomery, J. A., Jr.; Vreven, T.; Kudin, K. N.; Burant, J. C.; Millam, J. M.; Iyengar, S. S.; Tomasi, J.; Barone, V.; Mennucci, B.; Cossi, M.; Scalmani, G.; Rega, N.; Petersson, G. A.; Nakatsuji, H.; Hada, M.; Ehara, M.; Toyota, K.; Fukuda, R.; Hasegawa, J.; Ishida, M.; Nakajima, T.; Honda, Y.; Kitao, O.; Nakai, H.; Klene, M.; Li, X.; Knox, J. E.; Hratchian, H. P.; Cross, J. B.; Bakken, V.; Adamo, C.; Jaramillo, J.; Gomperts, R.; Stratmann, R. E.; Yazyev, O.; Austin, A. J.; Cammi, R.; Pomelli, C.; Ochterski, J. W.; Ayala, P. Y.; Morokuma, K.; Voth, G. A.; Salvador, P.; Dannenberg, J. J.; Zakrzewski, V. G.; Dapprich, S.; Daniels, A. D.; Strain, M. C.; Farkas, O.; Malick, D. K.; Rabuck, A. D.; Raghavachari, K.; Foresman, J. B.; Ortiz, J. V.; Cui, Q.; Baboul, A. G.; Clifford, S.; Cioslowski, J.; Stefanov, B. B.; Liu, G.; Liashenko, A.; Piskorz, P.; Komaromi, I.; Martin, R. L.; Fox, D. J.; Keith, T.; Al-Laham, M. A.; Peng, C. Y.; Nanayakkara, A.; Challacombe, M.; Gill, P. M. W.; Johnson, B.; Chen, W.; Wong, M. W.; Gonzalez, C.; Pople, J. A. *Gaussian 03*; Gaussian, Inc.: Pittsburgh, PA, 2003.

(32) (a) Baerends, E. J.; Ellis, D. E.; Ros, P. *Chem. Phys.* **1973**, *2*, 41. (b) te Velde, G.; Baerends, E. J. *J. Comput. Phys.* **1992**, *99*, 84. (c) te Velde, G.; Bickelhaupt, F. M.; Baerends, E. J.; Fonseca Guerra, C.; van Gisbergen, S. J. A.; Snijders, J. G.; Ziegler, T. *J. Comput. Chem.* **2001**, *22*, 931−.

(33) Baerends, E. J.; Autschbach, J.; Bérces, A.; Bo, C.; Boerrigter, P. M.; Cavallo, L.; Chong, D. P.; Deng, L.; Dickson, R. M.; Ellis, D. E.; Fan, L.; Fischer, T. H.; Fonseca Guerra, C.; van Gisbergen, S. J. A.; Groeneveld, J. A.; Gritsenko, O. V.; Grüning, M.; Harris, F. E.; van den Hoek, P.; Jacobsen, H.; van Kessel, G.; Kootstra, F.; van Lenthe, E.; McCormack, D. A.; Osinga, V. P.; Patchkovskii, S.; Philipsen, P. H. T.; Post, D.; Pye, C. C.; Ravenek, W.; Ros, P.; Schipper, P. R. T.; Schreckenbach, G.; Snijders, J. G.; Sola, M.; Swart, M.; Swerhone, D.; te Velde, G.; Vernooijs, P.; Versluis, L.; Visser, O.; van Wezenbeek, E.; Wiesenekker, G.; Wolff, S. K.; Woo, T. K.; Ziegler, T. *ADF2004.01, SCM, Theoretical Chemistry*; Vrije Universiteit: Amsterdam, The Netherlands, 2004.

(34) For recent reviews see: (a) Autschbach, J. In *Calculation of NMR and ESR Parameters. Theory and Applications*; Kaupp, M., Bühl, M., Malkin, V. G., Eds.; Wiley-VCH: Weinheim, 2004; p 227. (b) Autschbach, J.; Ziegler, T. In *Calculation of NMR and ESR Parameters, Theory and Applications*; Kaupp, M., Bühl, M., Malkin, V. G., Eds.; Wiley-VCH: Weinheim, 2004; p 249. (c) Autschbach, J. *Struct. Bonding* **2004**, *112*, 1.

(35) (a) van Lenthe E.; Baerends, E. J.; Snijders, J. G. *J. Chem. Phys.* **1994**, *101*, 9783. (b) van Lenthe, E.; van Leeuwen, R.; Baerends, E. J.; Snijders. J. G. *Int. J. Quantum Chem.* **1996**, *57*, 281−293. (c) van Lenthe, E.; Baerends, E. J.; Snijders, J. G. *J. Chem. Phys.* **1993**, *99*, 4597.

(36) van Lenthe, E.; Snijders, J. G.; Baerends, E. J. *J. Chem. Phys.* **1996**, *105*, 6505.

(37) In an adaption of the procedure described in ref 16a, $NiCl_2{\cdot}6H_2O$ was added to a solution of 7,8-$C_2B_9H_{12}^-$ (potassium salt) in strongly basic aqueous mediim (KOH). The resulting deep brown nickel(III) complex was extracted with diethyl ether. The organic phase was added to a solution of $FeCl_3{\cdot}6H_2O$ in water and stirred for 4 h. The diethyl ether layer was separated and evaporated to dryness, and the crude product was purified by column chromatography on silica gel with a CH_2Cl_2/hexane mixture as the eluent, affording give pure **3** ($R_f = 0.21$, 60% yield based on 7,8-$C_2B_9H_{12}^-$).

(38) (a) Fe: Kang, H. C.; Lee, S. S.; Knobler, C. B.; Hawthorne, M. F. *Inorg. Chem.* **1991**, *30*, 2024. Selected examples for Co: (b) QAJNAQ (ref-code in Cambridge Structure Database): Hardie, M. J.; Raston, C. L. *Angew. Chem., Int. Ed.* **2000**, *39*, 3835. (c) WEZHOY: Zuowei, X.; Jelínek, T.; Bau, R.; Reed, C. A. *J. Am. Chem. Soc.* **1994**, *116*, 1907. (d) BEVBUZ: Sinn, E.; Grimes, R. N. *Inorg. Chem.* **1982**, *21*, 1686. Selected examples for Ni: (e) NIDBOR: St. Clair, D.; Zalkin, A.; Templeton, D. H. *J. Am. Chem. Soc.* **1970**, *92*, 1173. (f) DINKOA, DINNAP, DINPIZ: Schubert, D. M.; Harwell, D. E.; Knobler, C. B.; Hawthorne, M. F. *Acta Chem. Scand.* **1999**, 53, 721.

(39) For a derivative bearing a metal-complexed indenyl substituent on one of the dicarbollides see: HAFDEX: Lewis, Z. G.; Welch, A. J. *J. Organomet. Chem.* **1992**, *438*, 353.

(40) It should be noted that the experimental numbers may be noticeably affected by packing effects, since for instance for the Co anion, where numerous X-ray crystal structures with different counterions and cocrystallized molecules are known, the respective distances can vary substantially from one crystal to the other, or from one dicarbollide unit to the other in case both are not equivalent due to a lower symmetry in the crystal.

(41) On the basis of observations made for the mixed-sandwich complex [Co(η^5-C_4H_4N)($C_2B_9H_{11}$)] it has recently been suggested that the parent cobalt bis(dicarbollide) **1** should prefer a cisoid arrangement (Viñas, C.; Llop J.; Teixidor, F.; Kivekäs R, Sillanpää, R. *Chem. Eur. J.* **2005**, *11*, 1933), a notion that is not supported by our results.

Table 1. Selected BP86-Optimized Geometrical Parameters [in Å and deg] for 1−3 and Their Rotamers

θ_{ideal}[a]	M[b]	θ[a]	M−C1	M−C2	M−B4	M−B7	M−B8	C1−C2	C1−B4	C2−B7	B4−B8	B7−B8	φ[i]
180	Fe	180.0	2.029	2.029	2.109	2.109	2.162	1.637	1.715	1.715	1.785	1.785	180.0
	expt[c]	*180.0*	*2.015*	*2.047*	*2.073*	*2.112*	*2.144*	*1.616*	*1.671*	*1.720*	*1.808*	*1.792*	*180.0*
	Co	180.0	2.027	2.027	2.112	2.112	2.160	1.639	1.721	1.721	1.792	1.792	180.0
	expt[d]	*180.0*	*2.024*	*2.017*	*2.111*	*2.082*	*2.141*	*1.632*	*1.708*	*1.717*	*1.786*	*1.775*	*180.0*
	Ni	180.0	2.051	2.051	2.134	2.134	2.182	1.642	1.735	1.735	1.809	1.809	180.0
	Ru	180.0	2.158	2.158	2.216	2.216	2.260	1.669	1.743	1.743	1.813	1.813	180.0
	Rh	180.0	2.165	2.165	2.223	2.223	2.262	1.663	1.744	1.744	1.818	1.818	180.0
	Pd	180.0	2.206	2.206	2.251	2.251	2.287	1.656	1.750	1.750	1.830	1.830	180.0
108	Fe	115.3	2.029	2.033	2.106	2.110	2.156	1.636	1.713	1.707	1.793	1.788	177.6
	Co	114.1	2.029	2.049	2.092	2.117	2.146	1.631	1.724	1.705	1.808	1.798	179.2
	expt[e,f]	*110.6*	*2.046*	*2.046*	*2.089*	*2.118*	*2.073*	*1.602*	*1.667*	*1.708*	*1.814*	*1.813*	*177.5*
	Ni	112.0	2.055	2.093	2.095	2.142	2.160	1.624	1.755	1.711	1.832	1.818	179.0
	Ru	133.4	2.156	2.167	2.219	2.221	2.261	1.663	1.742	1.741	1.816	1.812	178.2
	Rh	117.0	2.172	2.201	2.199	2.233	2.250	1.645	1.752	1.730	1.828	1.822	180.0
	Pd	94.7	2.241	2.284	2.205	2.264	2.276	1.609	1.786	1.740	1.845	1.832	179.2
36	Fe	43.8	2.030	2.033	2.107	2.108	2.156	1.639	1.713	1.712	1.794	1.792	175.9
	Co	41.2	2.045	2.052	2.094	2.108	2.131	1.627	1.721	1.713	1.811	1.809	178.2
	expt[g,f]	*37.9*	*2.040*	*2.049*	*2.084*	*2.099*	*2.106*	*1.624*	*1.698*	*1.698*	*1.822*	*1.776*	*179.0*
	Ni	38.3	2.089	2.106	2.097	2.128	2.128	1.612	1.744	1.721	1.846	1.841	178.2
	expt[h,f]	*36.1*	*2.068*	*2.075*	*2.086*	*2.105*	*2.118*	*1.606*	*1.731*	*1.708*	*1.838*	*1.830*	*179.5*
	Ru	64.0	2.169	2.182	2.209	2.226	2.256	1.660	1.741	1.734	1.819	1.816	177.4
	Rh	44.7	2.211	2.225	2.201	2.228	2.225	1.631	1.741	1.733	1.836	1.830	178.9
	Pd	39.4	2.286	2.303	2.212	2.253	2.227	1.609	1.759	1.735	1.871	1.853	174.8

[a] θ: dihedral angle B8′−M−B10−B8; θ_{ideal}: idealized value (see text). [b] Data for Co from ref 10. [c] NMe_4^+ salt, ref 38a. [d] Cyclotriveratrylene-complexed Na^+ counterions, ref 38b. [e] $[Ir(CO)(PPh_3)_3]^+$ counterion, ref 38c. [f] Mean values for two nonequivalent dicarbollide units or independent molecules in the unit cell. [g] $NHEt_3^+$ salt, numbering scheme adapted to the $\theta \approx -36°$ form in ref 38d. [h] Numbering scheme adapted to the $\theta \approx -36°$ form in ref 38e. [i] Angle B10−M−B10′.

Table 2. Relative Energies [kJ/mol] of Rotamers of 1−6 (BP86/AE1 level)

	θ_{ideal}[a]					
M	180°	108°	36°	144°	72°	0°
Fe	0.0	4.6	19.1	10.0	23.9	39.2
Co	0.0	1.6	10.6	15.2	24.0	36.5
Ni	8.4	2.0	0.0	24.1	21.7	27.7
Ru	0.0	2.8	14.1	3.6	14.3	25.4
Rh	0.0	0.3	4.5	4.9	8.0	14.6
Pd	17.9	8.0	0.0	20.8	9.3	10.3

[a] See footnote *a* of Table 1.

(compare the two plots at the top of Figure 1). For the Ni congener **3**, in contrast, the HOMO does not contain any d-character at the metal[42] and changes its nature upon rotation (compare the two lower plots in Figure 1). The bonding overlap between cluster MOs located at two opposing BB edges of both dicarbollide ligands, clearly visible in the plot labeled **3**(36°) in Figure 1, arguably contributes to the stabilization of this rotamer. The electronic structures of **1** and **3** with their large number of bonding MOs are complicated, however, and it is difficult to single out a particular factor that would clearly dominate either structural preference in **1** versus **3**.

In any event, in the whole set **1**−**6** the energetic preferences between the rotamers are not very pronounced, and the barriers between them are small to modest (see the three rightmost entries in Table 2). The highest barriers necessary to interconvert all rotamers of a given complex, between 8 and 24 kJ/mol,[43] are low enough to make rotation a fast process at ambient temperature, in particular on the NMR time scale.

Since full rotation over 360° also interconverts each rotamer with its respective enantiomer, the NMR spectra should show apparent C_{2h} (or C_{2v}) symmetry in all cases; that is, six signals are to be expected, three of which should have double intensity. This is essentially what is observed, save for unresolved closely spaced resonances or accidental degeneracies, which occur occasionally.[44] The computed chemical shifts, averaged assuming rapid rotation, are collected in Table 3, together with experimental data where available. In the case where no assignments were determined from 2D-NMR spectra, experimental numbers were assigned to atomic positions based on

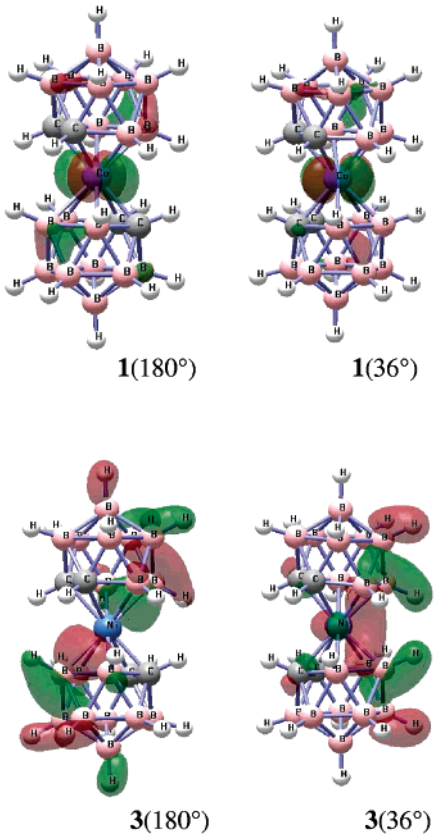

Figure 1. Plot of the HOMO for selected rotamers of **1** and **3** (BP86 level).

(42) The MO corresponding to that shown for **1**(180°) is lower in energy in **3**(180°), where it appears as HOMO−3.

(43) The second-highest from the barriers in Table 2.

(44) Review: Todd, L. J.; Siedle, A. R. *Prog. NMR: Spectrosc.* **1979**, *13*, 87.

Table 3. Chemical Shifts [in ppm] of 1−6 and Their Rotamers (GIAO-B3LYP/II′//BP86 level)[a] (in italics: experimental data, where available)

		nuclei						
M	σ_{ideal}	B(8)	B(10)	B(4,7)	B(9,12)	B(5,11)	B(6)	C(1,2)
Fe	180°	−4.7	−14.6	−10.6	−20.8	−30.5	−33.1	56.6
	expt[b]	*−5.7*	*≈ −14.0*	*≈ −14.0*	*≈ −14.0*	*−25.1*	*≈ −27.5*	
	108°	−0.8	−17.7	−11.6 (−12.3/−10.9)	−17.5 (−18.4/−16.6)	−29.4 (−31.1/−27.7)	−34.0	53.3 (54.3/52.4)
	36°	−1.5	−17.1	−9.8 (−9.6/−10.0)	−15.8 (−16.9/−14.6)	−30.4 (−31.1/−29.6)	−34.4	52.8 (50.3/55.4)
Co	180°	3.9	−2.4	−3.9	−9.5	−21.9	−26.0	61.1
	expt[c]	*5.8*	*0.9*	*−6.0*	*−6.6*	*−17.6*	*−23.0*	*51.9*
	108°	7.8	−3.0	−6.2 (−8.0/−4.3)	−9.0 (−9.8/−8.1)	−21.3(−23.1/−19.4)	−27.8	61.6 (62.7/60.4)
	36°	8.8	−3.2	−5.6 (−6.1/−5.0)	−7.3 (−8.7/−5.8)	−22.1(−22.9/−21.3)	−28.5	60.1 (58.2/61.9)
Ni	180°	20.2	20.3	7.0	0.7	−10.0	−18.3	79.7
	108°	23.3	18.5	5.1 (2.3/8.0)	1.8 (0.2/3.3)	−9.0 (−11.2/−6.8)	−20.0	77.6 (77.8/77.3)
	36°	26.4	16.8	3.0 (1.9/4.2)	3.7 (1.2/6.1)	−9.7 (−10.2/−9.1)	−20.5	74.4 (73.2/75.5)
	expt[d]	*20.2*	*15.9*	*2.2*	*2.2*	*−7.4*	*−16.6*	
	expt[e]	*21.6*	*16.9*	*3.6*	*2.9*	*−7.0*	*−16.3*	*69.0*
	expt[f]	*21.5*	*16.9*	*3.1*	*1.9*	*−7.8*	*−17.5*	*65.0*
Ru	180°	−5.7	−12.8	−9.9	−19.6	−30.1	−31.6	52.2
	108°	−3.7	−13.9	−12.0 (−12.5/−11.5)	−19.4 (−20.7/−18.2)	−29.2 (−30.1/−28.3)	−33.7	54.7 (52.7/56.7)
	36°	−2.5	−14.0	−10.3 (−12.0/−8.6)	−17.6 (−18.2/−17.0)	−30.5 (−31.7/−29.4)	−33.7	50.4 (48.2/52.6)
Rh	180°	1.4	−1.1	−4.9	−11.6	−22.6	−26.4	63.1
	108°	5.1	−2.1	−6.7 (−9.1/−4.4)	−10.8 (−11.8/−9.9)	−21.6 (−23.5/−19.7)	−28.2	62.2 (62.2/62.3)
	36°	7.9	−2.6	−6.6 (−8.1/−5.1)	−8.7 (−10.1/−7.4)	−22.3 (−23.2/−21.4)	−28.5	58.1 (56.3/59.9)
Pd	180°	15.6	17.1	4.6	−1.7	−11.4	−18.8	80.9
	108°	24.0	14.9	5.6 (0.5/10.7)	0.8 (−1.6/3.3)	−9.0 (−11.0/−6.9)	−20.5	75.0 (72.6/77.4)
	36°	27.1	14.4	2.1 (−0.5/4.6)	2.4 (0.5/4.2)	−9.7 (−10.5/−8.8)	−19.9	72.5 (71.8/73.2)
	expt[g]	*19.8*	*12.7*	*1.4*	*1.4*	*−8.7*	*−15.7*	

[a] Averaged assuming rapid rotation, where applicable (in parentheses: values in static minima); for the 4d metal complexes, B and C chemical shifts have been evaluated with the relativistic ECP on the metal. [b] Cs^+ counterion, MeCN, values quoted from ref 44. [c] Cs^+ counterion, ref 10. [d] Acetone, ref 16. [e] Acetone, this work. [f] $CDCl_3$, this work. [g] Benzene, values quoted from ref 44.

best accord between theory and experiment. In general, the pattern established for the Co parent is conserved for the other members in this series and is just shifted to lower field with decreasing charge of the complex.

For this larger set of complexes, slightly larger deviations between computed and observed $\delta(^{11}B)$ values are encountered than were found just for the Co representative **1**. Assuming that the observed spectra are dominated by the most stable minimum, the maximum and mean absolute deviations from experiment are 7.3 and 3.2 ppm, respectively. The former value (stemming from B(8) in **6**) is larger than the maximum error for **1**, ca. 4 ppm, and appears to be uncomfortably large for structural applications. The latter value, however, i.e., the overall accuracy, is similar to that achieved for **1**, 3.3 ppm.[10] It should be noted that some resonances can be quite sensitive to the rotation angle, θ, in particular for the neutral species with M = Ni and Pd. For the B(8) resonances in both complexes, which show the largest deviations in the whole set, population of the next-highest rotamer (with $\theta \approx 108°$) would result in a slight reduction of the maximum error.

3.2. Mixed- and Half-Sandwich Metal Dicarbollide Complexes. For the computed values of the Ru and Rh bis(dicarbollides) **4** and **5** in Table 3 no experimental data are known for direct comparison. Polyhedral borane and carborane clusters abound also with these metals, however, and numerous complexes have been prepared that contain one dicarbollide unit, together with other ligands.[45,46] We chose three representative examples from these complexes containing organic ligands such as aromatic π-donors or CO. Symmetrical co-ligands were chosen such as to limit the number of possible rotational isomers. Together with a corresponding iron complex[47] (which allows a comparison of the performance for a neutral mixed-sandwich complex with that for the bis(dicarbollide) ion **2**), these species constitute an additional, compact test set for further validation of our DFT methodology. This test set, which is well characterized structurally,[47,48] is sketched in Scheme 2. Geometrical parameters and chemical shifts for **7**−**10** are collected in Tables 4 and 5, respectively.

Scheme 2. Representative Mixed- and Half-Sandwich Dicarbollide Complexes (Cp* = permethylcyclopentadienyl)

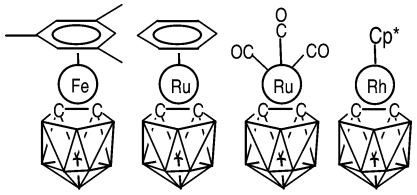

7 **8** **9** **10**

By and large, the computed ^{11}B chemical shifts for **7**−**10** reveal an accuracy similar to that for the bis(dicarbollides) discussed in the preceding section, with maximum and mean absolute deviations of 5.0 and 2.0 ppm, respectively. Interestingly, the calculations reveal that variation of the co-ligand L can have a large impact on the $\delta(^{11}B)$ values: for instance, on going from the $Ru(C_6H_6)$ to the $Ru(CO)_3$ fragment, the sequence

(45) For some selected examples with Ru see: (a) Behnken, P. E.; Hawthorne, M. F. *Inorg. Chem.* **1984**, *23*, 3420. (b) Cowie, J.; Reid, B. D.; Watmough, J. M. S.; Welch, A. J. *J. Organomet. Chem.* **1994**, *481*, 283. (c) Du, S. W.; Ellis, D. D.; Jelliss, P. A.; Kautz, J. A.; Malget, J. M.; Stone, F. G. A. *Organometallics* **2000**, *19*, 1983.

(46) For some selected examples with Rh see: (a) Fontaine, X. R.; Greenwood, N. N.; Kennedy, J. D.; Nestor, K.; Thornton-Pett, M.; Hermanek, S.; Jelinek, T.; Štíbr, B. *J. Chem. Soc., Dalton Trans.* **1990**, 681. (b) Jeffery, J. C.; Lebedev, V. N.; Stone, F. G. A. *Inorg. Chem.* **1996**, *35*, 2967. (c) Kudinov, A. R.; Perekalin, D. S.; Petrovskii, P. V.; Lyssenko, K. A.; Grintselev-Knyazev, G. V.; Starikova, Z. A. *J. Organomet. Chem.* **2002**, *657*, 115.

(47) BEXLAR: Hanusa, T. P.; Huffman, J. C.; Todd, L. J. *Polyhedron* **1982**, *1*, 77.

(48) (a) DEHFIF: Garcia, M. P.; Green, M.; Stone, F. G. A.; Somerville, R. G.; Welch, A. J.; Briant, C. E.; Cox, D. N.; Mingos, D. M. P. *J. Chem. Soc., Dalton Trans.* **1985**, 2343. (b) Refcode MEFNEQ in the Cambridge Structure Database, cited as: Ellis, D.; Jellis, P.; Stone, F. G. Private communication, 2000.

Table 4. Selected Distances for 7−10 [in Å],[a] BP86 Optimized and Observed in the Solid

no.	M(L)[b]	M−C1,2	M−B4,7	M−B8	C1−C2	C1−B4	B4−B8	M−C(L)
7	Fe(Mes)	2.059	2.118	2.154	1.625	1.712	1.802	2.126
	expt[c]	*2.066*	*2.110*	*2.125*	*1.624*	*1.726*	*1.788*	*2.122*
8	$Ru(C_6H_6)$	2.196	2.220	2.237	1.641	1.739	1.826	2.248
	expt[d]	*2.166*	*2.207*	*2.229*	*1.624*	*1.727*	*1.808*	*2.214*
9	$Ru(CO)_3$[e]	2.284	2.307	2.328	1.639	1.727	1.840	1.915
	expt[f]	*2.217*	*2.257*	*2.273*	*1.634*	*1.704*	*1.821*	*1.897*
10	$Rh(C_5Me_5)$	2.189	2.198	2.215	1.643	1.745	1.831	2.234
	expt[g]	*2.170*	*2.186*	*2.173*	*1.636*	*1.724*	*1.809*	*2.188*

[a] Mean values; unconstrained optimizations afforded approximate C_s symmetry in most cases. [b] Mes = 1,3,5-$C_6H_3Me_3$. [c] Reference 47. [d] Reference 48a. [e] With default convergence criteria, another, isoenergetic structure with the $Ru(CO)_3$ moiety rotated out of the symmetry plane can also be located. [f] $Ru(CO)_2(NCMe)$ derivative, ref 48b. [g] Reference 46a.

Table 5. Chemical Shifts [in ppm] of 7−10 (GIAO-B3LYP/II′//BP86 level)[a] (experimental data in italics)

	nuclei							
no.	B(8)	B(10)	B(4,7)	B(9,12)	B(5,11)	B(6)	C(1,2)	M(3)
7	5.1	−4.6	−8.8	−8.8	−23.4	−29.5	53.5	460
expt[b]	*3.6*	*−3.8*	*−8.3*	*−8.3*	*−19.9*	*−24.7*		
8	7.2	1.2	−6.3	−8.2	−21.0	−27.5	61.2	198
expt[c]	*2.8*	*1.3*	*−6.7*	*−8.2*	*−18.6*	*−23.2*		
9	−2.0	11.3	−8.2	−3.4	−19.8	−19.3	55.5	406
expt[d]	*−3.7*	*8.7*	*−8.9*	*−5.0*	*−17.8*	*−17.8*		
10	13.6	−1.0	−2.8	−8.5	−21.1	−27.8	63.0	180
expt[e]	*8.6*	*−1.8*	*−3.5*	*−8.3*	*−18.6*	*−23.4*		

[a] Averaged to exact C_s symmetry; for the 4d metal complexes, B and C chemical shifts have been evaluated with the relativistic ECP on the metal, whereas the metal shifts, given relative to the respective metallocenes, have been obtained with an all-electron basis (see Computational Details). [b] $CDCl_3$, ref 47. [c] *p*-Cymene [1,4-C_6H_4(Me)(*i*-Pr)] derivative, $CDCl_3$, ref 45b. [d] Acetone, ref 45a. [e] CD_2Cl_2, ref 46a.

of the ^{11}B resonances for B(8), B(10), B(4,7), and B(9,12) is completely reordered (see first four entries for **8** and **9** in Table 5).[49]

When all *closo*-dicarbollide complexes **1**−**3** and **6**−**10** are evaluated together, the maximum and mean absolute deviations from experiment are 7.3 and 2.6 ppm, respectively, over a total range of ca. 50 ppm. The performance of the GIAO-B3LYP level is illustrated in Figure 2, a plot of computed versus experimental $\delta(^{11}B)$ values.

As can be inferred from the scatter of the data points in this plot, the overall performance of the particular DFT variant is only fair and is noticeably inferior to that of conventional ab initio methods for metal-free carboranes.[6a] The corresponding conclusions based on the data for **1**[10,50] are thus borne out for this larger set of compounds. Moreover, a linear regression of calculated versus experimental data affords a slope of 1.19, i.e., significantly larger than unity.[51] This shortcoming is not remedied by switching to another density functional in the NMR part. In fact, when the same "pure" BP86 functional from the geometry optimization is used in the NMR computation instead of the hybrid B3LYP variant, very similar results are obtained (see Tables S1 and S2 in the Supporting Information). Specifically, maximum and mean absolute deviations of 6.8 and 2.9 ppm, respectively, are obtained at the GIAO-BP86/II′ level, with a slope of 1.19 for the linear fit. The performance of BP86 and B3LYP is thus very similar as far as ^{11}B chemical shifts are concerned. A similarly small sensitivity of the computed $\delta(^{11}B)$ values toward the particular density functional had already been noted for **1**.[10] This finding is potentially useful for further applications, as the coupling terms arising from the Hartree−Fock exchange make the shielding computations with hybrid functionals somewhat more expensive than with "pure" functionals (by about a factor of 2 for the complexes of this study). For consistency with previous work we will continue to discuss GIAO-B3LYP results for the remainder of this paper.

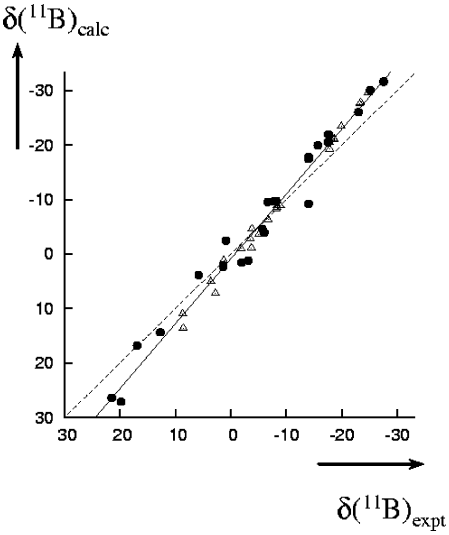

Figure 2. Plot of calculated (GIAO-B3LYP/II′) vs experimental ^{11}B chemical shifts for bis(dicarbollides) **1**−**3** and **6** (black circles) and mono-dicarbollides **7**−**10** (open triangles); solid line: linear fit; dashed line: ideal slope.

^{13}C chemical shifts of dicarbollide complexes are sparse and, to our knowledge, have not been known for any of the species of this study, except for **1**. We have now measured the ^{13}C NMR spectrum of the Ni analogue **3** (see Table 3 for the data); as with the results for **1**,[10] the computed $\delta(^{13}C)$ values for **3** are too high by ca. 10 ppm. A quantitative assessment is hampered by the fact that the computed and experimental $\delta(^{13}C)$ data depend noticeably on the conformation and on the solvent, respectively. It seems likely, however, that the ^{13}C chemical shifts predicted for the other complexes of this study will be overstimated to a similar extent.

Likewise, no transition-metal resonance of any dicarbollide complex has been reported yet. Among the metal nuclei in this

(49) The large downfield shift of the remote (antipodal) B(10) resonance on going from **8** to **9** is noteworthy. Apparently, the increased π-backbonding from the metal to the CO ligands as compared to benzene makes the whole metal fragment more electronegative; similar remote shifts produced by electronegative elements in borane cages are well known as the "antipodal effect", cf.: Bühl, M.; Schleyer, P. v. R.; Havlas, Z.; Hnyk, D.; Hermanek, S. *Inorg. Chem.* **1991**, *30*, 3107, and references therein.

(50) It should be recalled at this point that at the simplest conventional ab initio level, Hartree−Fock, very poor chemical shifts are obtained for **1**, cf. ref 10.

(51) Occasionally, DFT predicts too strong deshielding also for other nuclei bonded to transition metals; see for example: (a) Kaupp, M.; Malkin, V. G.; Malkina, O. L.; Salahub, D. R. *Chem. Phys. Lett.* **1995**, *235*, 382. (b) Ruiz-Morales, Y.; Schreckenbach, G.; Ziegler, T. *J. Phys. Chem.* **1996**, *100*, 3359. The so-called Malkin correction (in an SOS-DFPT scheme), which is beneficial for many main-group compounds, is indicated to affect ligand shifts only marginally, cf.: (c) Wilson, P. J.; Amos, R. D.; Handy, N. C. *Phys. Chem. Chem. Phys.* **2000**, *2*, 187.

Scheme 3. Pd(d^8) Dicarbollide Half-Sandwich Complexes

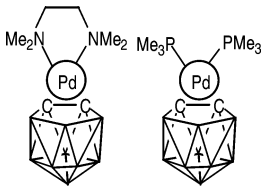

11 **12**

study, ^{57}Fe, ^{99}Ru, and ^{103}Rh would appear (besides ^{59}Co)[10] as the best candidates for eventual detection.[52] We include the chemical shifts of these nuclei[53] as predictions in Table 5. For comparison, the computed metal shifts in the most stable rotamers of **2**, **4**, and **5** are $\delta(^{57}\text{Fe}) = 433$, $\delta(^{99}\text{Ru}) = 25$, and $\delta(^{103}\text{Rh}) = 148$, respectively. Replacement of one dicarbollide moiety in these complexes with other π-ligands thus results in noticeable downfield shifts for the central metal nuclei.

The Ni and Pd centers in **3** and **6** carry high formal oxidation states (+IV)[54] and are readily reduced, taking up one or two electrons. For dicarbollide half-sandwich complexes with Pd, the formal oxidation state II with d^8 configuration at the metal is actually the clearly preferred one. In keeping with the electron count according to Wade's rules[55] and the propensity of d^8 Pd complexes for a square-planar coordination mode, the hapticity in the resulting $Pd^{II}(C_2B_9H_{11})$ fragments is usually closer to three than to five, and the *closo* cage found for the d^6 species **6** opens up siginificantly. The extent of this cage-opening, however, can depend strongly on the nature of the co-ligands attached to Pd.[56] Our initial attempts to extend our studies to two representative $[Pd(L_2)(C_2B_9H_{11})]$ complexes (Scheme 3) met with surprisingly limited success: Deviations in $\delta(^{11}\text{B})$ values as large as ca. 10 and 18 ppm were encountered for **11** and **12**, respectively (for B(8), to lower field, in both cases). According to ZORA calculations (see below), inclusion of spin−orbit coupling does not reduce these exceptionally large errors. In part, these errors may arise from shortcomings of the optimized geometries, which show unusually large overestimations of the Pd−C(1,2) distances (on the order of 0.1−0.2 Å for **11** and **12**, respectively), possibly due to the failure of present-day functionals to properly account for attractive dispersion interactions between these electron-rich sites. It is unlikely that inclusion of solvation effects would improve the results, as we had shown that the computed $\delta(^{11}\text{B})$ values of **1** are little affected by embedding the pristine ions in a polarizable continuum.[10] We defer a deeper analysis of these preliminary results to a systematic study of *nido*-metallacarboranes and note that the fair performance of our computational approach, as illustrated in Figure 2, may be restricted to *closo* species. With this caveat in mind, we now turn to a structural application in a topical area of metallacarborane chemistry.

Scheme 4. 14-Vertex Model Complex with Numbering Scheme (aromatic ligands and H atoms not shown)

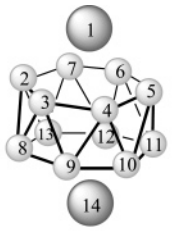

= BH, CH

= Ru(C_6H_6)

Isomer	C at position
13a	2,8
13b	2,9
13c	2,10

3.3. Structural Application: 14-Vertex Metallacarborane. Expanding the limits of icosahedral and supraicosahedral heteroborane chemistry by synthesizing ultralarge boron polyhedra with more than 14 vertices has been named as one of the challenges for "metallacarboranes in the new millenium".[57] While the first 14-vertex carborane has been characterized only recently,[58] 14-vertex metallacarboranes have been known for a longer time.[59] Formally derived from hypothetical D_{6d}-symmetric $[B_{14}H_{14}]^{2-}$,[60] this long-established, yet small family has recently been enlarged by new members of the homo- and heterobimetallic type,[61] two of which were structurally characterized by X-ray crystallography. In both cases the metal fragments are located on opposite vertices of a bicapped hexagonal antiprism (1,14 position). In the case of {(*p*-cymene)-Ru}$_2C_2B_{10}H_{12}$, the position of the C atoms in the carborane framework could not be refined from the X-ray data. According to the ^{1}H and ^{11}B NMR spectra, this complex is symmetric,[61] and (2,8), (2,9), or (2,10) positions for the C atoms would be compatible with the spectra (see Scheme 4 for numbering). A plausible choice between these alternatives can be based on the structure of a related (Ru,Ni) heterobimetallic complex, where the C atoms could be located at the (2,10) positions. We were interested to see if NMR calculations could support this assignment also for the Ru homobimetallic species. To this end, we have pruned the *p*-cymene ligand to its benzene core and optimized the three isomeric model candidates **13a**−**c** (Scheme 4).

Comparison of the optimized bond distances in these models with those found in the solid in order to assign the isomer is inconclusive, also in light of the rather large uncertainties of the refined bond distances (standard deviations between 0.01 and 0.02 Å for distances between nonmetal atoms in the cage).[61] The (2,8) isomer **13a** appears to be disfavored because it has a rather short bond between the two adjacent carbons, 1.621 Å (BP86 level), which has no counterpart in the observed structure in the solid: the shortest inter-rim distance in the latter is 1.681-(11) Å, which agrees much better with the corresponding C−B

(52) See for example: *Transition Metal Nuclear Magnetic Resonance*; Pregosin, P. S., Ed.; Elsevier: Amsterdam, 1991.

(53) For comparative purposes, we report the metal shifts relative to the respective metallocenes, $M(C_5H_5)_2^n$. For conversion to the usual standards, neat $Fe(CO)_5$, aqueous $K_4[Ru(CN)_6]$, and a standard resonance frequency Ξ for ^{57}Fe, ^{99}Ru, and ^{103}Rh, respectively, one may add the experimental shifts for the metallocenes, which are (relative to these standards) $\delta = 1532$, -1270, and -1839 for the metal nucleus in $Fe(C_5H_5)_2$, $Ru(C_5H_5)_2$, and $Rh(C_5H_5)_2^+$, respectively (taken from ref 52).

(54) It should be noted that these formal charges do not reflect the actual electron distribution; for example, for the Ni atom in **3**(36°) an NPA charge of +0.67 is obtained at the B3LYP/II′ level, much smaller than the formal value, +4.

(55) (a) Wade, K. *Adv. Inorg. Chem. Radiochem.* **1976**, *18*, 1. (b) Mingos, D. M. P. *Acc. Chem. Res.* **1984**, *17*, 311.

(56) Colquhoun, H. M.; Greenhough, T. J.; Wallbridge, M. G. H. *J. Chem. Soc., Dalton Trans.* **1985**, 761.

(57) Grimes, R. N. *Coord. Chem. Rev.* **2000**, *200*−*202*, 773−811.

(58) Deng, L.; Chan, H.-S.; Xie, Z. *Angew. Chem., Int. Ed.* **2005**, *44*, 2128−2131.

(59) For selected examples see: (a) Evans, W. J.; Hawthorne, M. F. *J. Chem. Soc., Chem. Commun.* **1974**, 38. (b) Maxwell, W. M.; Bryan, R. F.; Grimes, R. N. *J. Am. Chem. Soc.* **1977**, *99*, 4008. (c) Maxwell, W. M.; Bryan, R. F.; Sinn, E.; Grimes, R. N. *J. Am. Chem. Soc.* **1977**, *99*, 4016. (d) Grimes, R. N. *Acc. Chem. Res.* **1978**, *11*, 420.

(60) Schleyer, P. v. R.; Najafian, K.; Mebel A. M. *Inorg. Chem.* **1998**, *37*, 6765.

(61) Ellis, D.; Lopez, M. E.; McIntosh, R.; Rosair, G. M.; Welch, A. J. *Chem. Commun.* **2005**, 1917.

Table 6. BP86-Optimized Mean Bond Distances for 13a−c, Together with Experimental Data for the *p*-Cymene Derivative (no C atoms located, see text)

cage bond	2,8 (**13a**)	2,9 (**13b**)	2,10 (**13c**)	*expt*[a]
Ru−rim	2.278	2.279	2.279	*2.249(9)*
within rim	1.762	1.759	1.759	*1.710(13)*
inter-rim	1.753	1.750	1.748	*1.723(14)*

[a] Reference 61.

distances computed for the carbon-apart isomers **13b** and **13c**, 1.69−1.70 Å. The mean bond distances involving metal and all rim atoms (which are the only ones that can be compared directly with the X-ray structure where B and C could not be discerned) are very similar for all three isomers (Table 6) and cannot be used to distinguish between them.

The computed ^{11}B chemical shifts, on the other hand, are much more sensitive to the positions of the C atoms on the cage. The experimental spectrum, 4 lines (one of which with double intensity due to accidental overlap) in the narrow range between −16.1 and −25.6 ppm, is best reproduced by the computed values for **13c** (see B3LYP data in Table 7). Isomer **13a** can be excluded because it has a resonance computed at −2.8 ppm, more than 13 ppm downfield from the most deshielded experimental signal. Likewise, the pattern for isomer **13b** cannot be reconciled with experiment, as the two closest resonances expected to merge into the double-intensity signal are predicted around −8.3 ppm, whereas the corresponding peak is observed at −20.7 ppm, i.e., off by more than 12 ppm. In both cases, the deviations from experiment would be much larger than the maximum deviation (ca. 7 ppm) encountered for the *closo* species assessed in the preceding section, and the occurrence of either **13a** or **13b** can safely be excluded. These large deviations and, in contrast, the good agreement of the NMR spectrum computed for **13c** with that observed experimentally are illustrated in Figure 3.

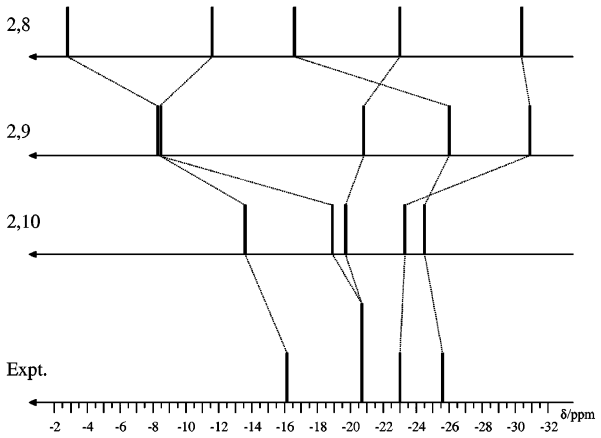

Figure 3. Schematic representations of the B3LYP/II′-computed ^{11}B NMR spectra of **13a**, **13b**, and **13c** (from the top, labeled according to the C positions), together with that of the experimental one for the *p*-cymene derivative (data from ref 61).

When the NMR nuclei under scrutiny are bonded to heavier elements, relativistic effects can come to the fore.[34,62] A certain part of the latter, the so-called scalar relativistic effects, can implicitly be taken into account even in an otherwise nonrelativistic calculation, namely, by using a relativistically adjusted ECP on the heavy metal[63] (as we have done in our B3LYP/II′ level). It is well known, however, that a heavy neighbor can strongly affect the NMR properties of a given NMR nucleus by way of a different sort of relativistic effect, namely, spin−orbit (SO) coupling, which is relayed by a Fermi-contact mechanism that is now well understood.[64] The magnitude of such SO effects can depend on the particular bonding situation and tends to increase steeply with the mass of the heavy atom. For 5d transition-metal complexes, SO effects can actually be of paramount importance.[34,65] But also for nuclei bonded to 4d metals, noticeable SO effects have been found, e.g., up to 16 ppm for the ^{15}N chemical shifts of aromatic N-donors attached to Ru.[66] To estimate the extent of such effects on $\delta(^{11}B)$ in metallaboranes, we have performed explicit relativistic NMR calculations employing the ZORA-SO methodology, which is well suited for this purpose.[34] The results for **13a−c** are included in Table 7 (values in parentheses). Only minor changes from the scalar relativistic B3LYP data are found, and part of these changes are rather due to the different functional employed in both calculations, B3LYP versus BP86. The actual SO corrections at the ZORA level (which are shielding throughout) do not exceed 1.5 ppm for any ^{11}B nucleus in these complexes.[67] Similarly small effects are obtained for the Pd species **11** and **12** mentioned above.

In summary, both scalar and SO relativistic NMR calculations for model compound **13** unambiguously demonstrate that it is indeed the 1,14,2,10-isomer of $\{(p\text{-cymene})Ru\}_2C_2B_{10}H_{12}$ that has been isolated and that other possible candidates with different C atom locations can safely be excluded.[68]

Conclusions

We have presented a systematic density functional study of *closo* transition-metal dicarbollide complexes, comprising symmetrical metal bis(dicarbollides), $[3\text{-M-}(1,2\text{-}C_2B_9H_{11})_2]^n$ (**1**−**6**), and selected mixed- or half-sandwich complexes $[3\text{-M(L)-}(1,2\text{-}C_2B_9H_{11})]$ (**7**−**10**). The bis(dicarbollides) are all characterized by three different rotamers with staggered conformation of the two dicarbollide moieties, separated by three distinct, eclipsed transition states. The minima are close in energy and the barriers between them are low (below 40 kJ/mol at the BP86 level), consistent with facile rotation about the long molecular axis. While the minimum with transoid arrangement of the two dicarbollide moieties is preferred for M = Fe, Co, Ru, and Rh, a cisoid conformation is slightly more stable for M = Ni and Pd, in accordance with experimental observations.

Special attention is called to the accuracy of the ^{11}B chemical shifts computed with well-established DFT procedures. For the test set **1**−**10**, the mean absolute deviation of the GIAO-B3LYP/II′-computed $\delta(^{11}B)$ values from experiment is lower than 3 ppm, but errors for individual resonances can be as large as 7 ppm. The computed $\delta(^{11}B)$ values are little affected (by less than 2 ppm typically) when a different density functional is

Table 7. GIAO-B3LYP ^{11}B Chemical Shifts of 13a−c (in ppm; in parentheses: ZORA-SO/BP86 values)

isomer	B3	B4	B5	B6	B7
2,8 (**13a**)	−23.0 (−25.1)	−11.6 (−13.1)	−2.8 (−6.4)	−16.6 (−17.4)	−30.4 (−32.0)
2,9 (**13b**)	−20.9 (−22.9)	−8.4 (−10.0)	−8.3 (−11.1)	−26.0 (−27.0)	−30.9 (−32.0)
2,10 (**13c**)	−19.7 (−21.8)	−13.6 (−14.4)	−18.9 (−21.7)	−24.5 (−25.1)	−23.3 (−24.6)
expt[a]	*−20.7*	*−16.1*	*−20.7*	*−25.6*	*−23.0*

[a] *p*-Cymene derivative, $CDCl_3$, ref 61.

employed in the NMR part (specifically, BP86 instead of B3LYP) or, for selected 4d complexes, when relativistic spin−orbit effects are explicitly taken into account. In general, substituent effects on $\delta(^{11}B)$ appear to be overestimated to some extent at the DFT levels employed, as evidenced by the linear fit of computed versus experimental chemical shifts, which affords a slope of 1.2 instead of the ideal value, 1. Thus, the performance of standard DFT methods for the *closo*-metallacarboranes **1**−**10** falls somewhat short of that of conventional ab initio methods for metal-free heteroboranes.

Nonetheless, the accuracy achievable for the metallacarboranes can be sufficient for structural applications in favorable cases, i.e., when the structural candidates that can give rise to an observed NMR spectrum differ significantly in their computed chemical shifts. We have presented a showcase example for such an application, namely, for a 14-vertex bimetallic *closo*-ruthenacarborane. The precise location of the carbon atoms on the carborane cluster of $\{(p\text{-cymene})Ru\}_2C_2B_{10}H_{12}$, for which only circumstantial experimental evidence had existed so far, has been verified conclusively by NMR computations for salient isomeric model complexes.

Thus, DFT-based NMR computations emerge as a promising structural tool for the huge family of *closo*-metallacarboranes, even though the confidence level of such assignments and refinements is somewhat lower than it is in the case of metal-free heteroboranes, where ab initio-calculated ^{11}B chemical shifts are associated with a smaller uncertainty. Further investigations exploring the limits, and exploiting the potential, of chemical-shift calculations for metallaheteroboranes should be rewarding.

Acknowledgment. This work was supported by the German Academic Exchange Service (DAAD) and the Academy of Sciences of the Czech Republic in the joint PPP program, as well as the Ministry of Education of the Czech Republic (project no. LC 523). M.B. wishes to thank Prof. W. Thiel and the MPI in Mülheim for continuous support.

Supporting Information Available: Optimized coordinates of all species **1**−**13** discussed in the text, and Tables S1 and S2 with GIAO-BP86/II′-computed chemical shifts. This material is available free of charge via the Internet at http://pubs.acs.org.

OM051025F

(62) For selected reviews see: (a) Kaupp, M.; Malkin, V. G.; Malkina, O. L. In *The Encyclopedia of Computational Chemistry*; Schleyer, P. v. R., Allinger, N. L., Clark, T., Gasteiger, J., Kollman, P. A., Schaefer, H. F., III; Schreiner, P. R., Eds.; Wiley: Chichester, 1998; p 1857. (b) Schreckenbach, G.; Ziegler, T. *Theor. Chem. Acc.* **1998**, *99*, 71. (c) Reference 29b.

(63) For instance ref 51a and: Kaupp, M.; Malkin, V. G.; Malkina, O. L.; Salahub, D. R. *J. Am. Chem. Soc.* **1995**, *117*, 1851.

(64) See for instance: Kaupp, M.; Malkina, O. L.; Malkin, V. G.; Pyykkö, P. *Eur. J. Chem.* **1998**, *4*, 118.

(65) See for instance: (a) Gilbert, T. M.; Ziegler, T. *J. Phys. Chem. A* **1999**, *103*, 7535. (b) Schreckenbach, G.; Wolff, S. K.; Ziegler T. *J. Phys. Chem. A* **2000**, *104*, 8244.

(66) Ramalho, T. C.; Bühl, M. *Helv. Chim. Acta* **2005**, *88*, 2705.

(67) According to natural bond orbital analysis (ref 23), the (multicenter) bonds between Ru and the carborane moiety are characterized by essentially pure d-orbital contributions from the metal, with little or no s-character. Thus, an efficient Fermi-contact interaction between Ru and adjacent B atoms is precluded, which would be the principal mechanism for the transfer of SO effects on nuclear shieldings, cf. ref 64.

(68) Incidentally, of the possible forms **13a**−**c** considerd, the 2,10-isomer **13c** is also the most stable one thermodynamically, 12.8 and 74.3 kJ/mol below **13b** and **13a**, respectively.